Preferred citation: A. Bugiel, F. Hähnel, K. Wolf, J. Strauß and T. Kuntzsch. Enhanced test devices for the development of novel paper-like materials for sandwich-structures. In **Advances in Pulp and Paper Research, Oxford 2017**, *Trans. of the XVIth Fund. Res. Symp. Oxford, 2017*, (W. Batchelor and D. Söderberg, eds), pp 27–41, FRC, Manchester, 2018. DOI: 10.15376/frc.2017.1.27.

ENHANCED TEST DEVICES FOR THE DEVELOPMENT OF NOVEL PAPER-LIKE MATERIALS FOR SANDWICH-STRUCTURES

Alexander Bugiel[1], Falk Hähnel[1], Klaus Wolf[1], Johann Strauß and Timo Kuntzsch[3]

[1] Institute of Aerospace Engineering, Technische Universität Dresden, Germany
[2] Papiertechnische Stiftung Munich, Germany
[3] Papiertechnische Stiftung Heidenau, Germany

ABSTRACT

High performance sandwich components have a great significance in aerospace applications. Particularly, lightweight sandwich structures made of honeycomb or foldcores show excellent load carrying capabilities. Both types of cores are usually made of aramid paper coated with phenolic resin. Therefore, the development of improved paper-like materials seems to be a promising approach to improve the mechanical performance of this kind of cores. An essential part of this development process is the evaluation of the new materials by the complete characterisation of the mechanical properties. This is still a challenging task, since the resulting papers are orthotropic and most of the existing testing procedures and devices are not suitable for very thin sheet materials. This is particularly true for investigating stiffness and strength properties under compressive and shear loading.

The paper presents a novel single-curved compression test device as well as an adapted shear-frame for the in-plane characterisation of very thin specimens. These devices have been applied in the development process of a new paper-like material that consists of three layers in order to increase the stiffness and strength of honeycomb- and foldcores. The

performance of this material was evaluated by comparing relevant mechanical properties to that of state of the art paper materials. Based on the experimental results the benefits of the new paper-like material could be shown.

1 INTRODUCTION

Honeycomb- and foldcores used in aerospace sandwich structures are made of relatively thin materials like NOMEX® and KEVLAR® papers coated with phenolic resin. The walls of such kind of cores have relatively large unsupported areas. Hence, buckling of the cell walls is the typical failure mode under shear and compressive loads on the core. A common approach to raise the buckling loads is to coat the basic cell-wall material with one or more layers of resin in order to increase the bending stiffness [1]. Due to the high density of the phenolic resin, this measure does not result in a significant improvement of the strength to weight ratio of the core. Using smaller cell sizes is also a typical option, but that leads to a decreasing strength to weight ratio [2].

Another approach to improve the bending stiffness of the walls is to modify the cross-section geometry by crimping the material. Investigations by Zakirov *et al.* [3] showed that the benefit of the increased area moment of inertia is almost equal to the loss in stiffness caused by damages forming in the wall material during the crimping process. Therefore, the strength to weight ratio does not increase.

An alternative approach is to develop paper-like materials having an increased bending stiffness. To compare the newly developed with state of art paper materials, it is necessary to characterize their performance under tensile, compressive and shear loads. For some of these material properties no suitable test methods or appropriate devices were available. Hence, a novel compression test device was developed and a shear-frame adapted for the characterization task.

2 PAPER DEVELOPMENT

Main requirements for the development of improved paper-like materials for core structures have been non-combustibility and an increased bending stiffness. Step one in the development process was the production of material variations in the laboratory. A screening was performed in order to test the suitability of a broad range of different potentially usable pulps for sheet forming. As a result, paper materials modified with fibres that offer good sheet forming, formation as well as strength properties, for example aramid and carbon, were identified.

Based on the obtained results sheet forming tests were carried out in the second step. This investigation included the application of lightweight fillers. The aim was to increase the paper volume without weight gain. Fillers such as Expancel® or Perlit® make it possible to raise the specific volume of sheets. However, this measure does not necessarily lead to a higher bending stiffness, since the use of fillers reduces the static strength of non-impregnated sheets.

Using these findings, various test series were performed in a third phase with promising pulp and fibre/filler systems to obtain multi-layer sheets in the laboratory. The aim of the experiments was to improve the bending stiffness by combining stiff and high-strength face layers with a lightweight, voluminous middle layer to create multi-layer paper structures. Continuous processes have been identified which enable the production of three-layer paper materials with a grammage of around 150 g/m^2 in the laboratory. The continuously produced paper shows a significant orthotropic behaviour that is beneficial for core applications.

Furthermore, for three-layer materials containing carbon fibres impregnated with phenolic resin an improved weight-specific bending stiffness could be demonstrated. An example is shown in the cross-sectional image in Figure 1.

Due to non-combustibility and good mechanical performance, an adapted paper-like material (APM) has been selected from the examined samples. Table 1 shows the composition of this material. Whereas the base paper has low mechanical properties, the phenolic resin impregnated paper shows a promising mechanical behaviour and has a grammage of 366 g/m^2.

To demonstrate the advantage of APM over state of the art paper-like materials used in honeycomb- or foldcores, it was necessary to determine and compare the mechanical properties. For this purpose, N636® from DuPont has been chosen as the benchmark material. It consists of para-aramid fibres and fibrids and is calendered and coated with phenolic resin. The weight proportion of phenolic resin is 50 % and the grammage is 166 g/m^2.

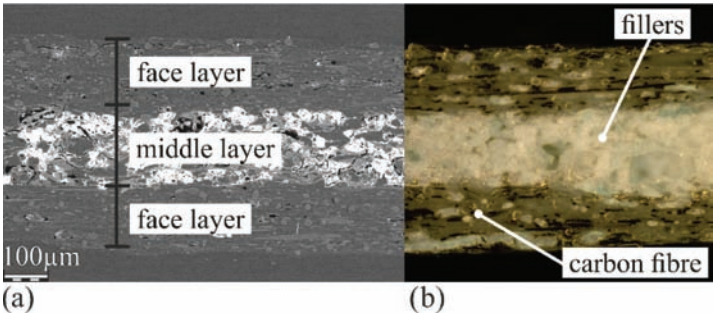

Figure 1. SEM and light microscopic cross section image of a three-layer paper.

Table 1. Composition of the adapted paper-like material (APM)

	Fibres	*Filler*
Face layer	60% aramid fibrids and 40 % carbon fibres	–
Middle layer	60% aramid fibrids and 10 % carbon fibres	Perlit® 30%

3 TEST DEVICES

For a complete in-plane characterisation of orthotropic materials tensile and compression tests in machine- and cross-direction of the sheets as well as shear tests had to be carried out. Since the standard ISO 1924–2 [4] is adequate for tension testing of paper-like materials, only compression and shear test procedures and devices had to be developed.

3.1 Compression test – single-curved test device

Most paper materials show not the same behaviour under in-plane compressive and in-plane tensile loads. While the linear elastic regime is similar, the yielding and maximum strength varies [5]. Therefore, a variety of different test methods and devices has been developed. Most of them are summarised by Mark *et al.* in [6]. They can be divided into two main groups.

The first group comprises of test methods using specimen, which are curved in the non-loaded direction. Examples are the ring crush test [7], the IPC modified ring crush test [8], the FPL support cylinder test [6] and the corrugated medium test [9]. Caused by the curved specimen geometry, the transverse elongation will always result in an out-of-plane deformation. Hence, most of these test methods use short spans to prevent premature buckling. The constrained transversal elongation also results in a biaxial state of stress. Therefore, the mechanical parameters required for numerical simulations cannot be determined by this kind of experiments.

Test methods that use plane specimens can be further divided into two subgroups. The compression test proposed by S. Calvin and C. Fellers [10] as well as the concora liner test [11] use short span specimens. They suffer from the same disadvantages as other short span tests. The second subgroup comprises test methods using long span specimens. Most of these tests have lateral supports on both sides: STFI solid support test [12], STFI blade support test [10], FPL lateral support test [13] and PPRIC plate support test [14]. Since the specimens are not visible during testing, their deformation can only be calculated from the external

displacements. Furthermore, the clamping forces of the support plates have a significant influence on the results [6], leading to a limited repeatability.

The FPL vacuum restrained test [13], [15] works with a specimen that is supported by thin rods. An elastic layer holds them in place and enables the tip to move freely in the in-plane directions, but not in the out-of-plane direction. A vacuum holds the specimen on the tip of the rods. Since one side of the specimen is visible, digital image correlation methods can be applied during testing. The disadvantages of this method are the complexity and the vacuum that deforms the specimen and can influence the failure behaviour.

3.1.1 Developing a single-curved test device

Since the available test methods proved not suitable for the given task, a new test device has been developed. The first important criterion was to obtain a uniaxial state of stress in the test specimen. Hence, a mean free path ratio of at least five has been defined. As a result, a lateral support is necessary. To retain a visible surface for digital image correlation, a one-sided lateral support was selected. A single-curved concave surface assures that the specimen is adequately supported, see Figure 2.

The function $w(x)$ for the curvature was determined by the static Euler-Bernoulli beam equation:

$$M(x) = -EI\frac{d^2w(x)}{dx^2} \tag{1}$$

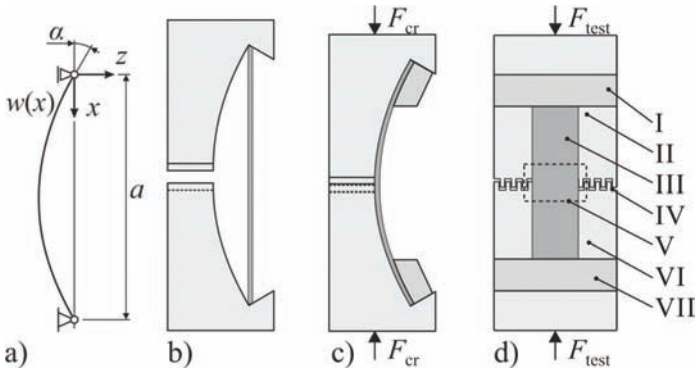

Figure 2. Theory and construction of the single-curved test device: (a) definition of the deflection curve and the boundary conditions; (b) test device with unbended specimen; (c) test device with bended specimen (III) and clamping brackets (I, VII); (d) the front view shows the comb system (IV) between the upper support plate (II) and the bottom support plate (VI) and the evaluation area (V).

According to Figure 2(a), the following boundary conditions are valid:

$$w(0) = 0 \tag{2}$$

$$w(a) = 0 \tag{3}$$

$$\frac{dw(0)}{dx} = \tan(-\alpha) = m_0 \tag{4}$$

$$M(x) - F_{cr}\, w(x) = 0 \tag{5}$$

As a result, the deflection curve $w(x)$ yields as

$$w(x) = \frac{m_0 a}{\pi} \sin\left(\frac{\pi}{a} x\right) \tag{6}$$

where m_0 is the deflection angle and a is the distance between the specimen endpoints. Equation (6) shows that the deflection is independent of material parameters like the stiffness and the thickness. Nevertheless, both the resultant force F_{cr} in direction of loading

$$F_{cr} = \frac{\pi^2 EI}{a^2} \tag{7}$$

and the maximum bending stress

$$\hat{\sigma}_B = \frac{\pi E t m_0}{2a} \tag{8}$$

depend linearly on the material stiffness E and sheet thickness t. Note that the maximum bending stress $\hat{\sigma}_B$ is not the maximum stress that occurs in the specimen. It is calculated from F_{cr} an idealised value that is much higher than the real critical force. Investigations have shown that m_0 and a have to be chosen in such a way that the maximum bending stress is 5 to 50% of the maximum tensile stress. Higher values can cause a combined bending-compression failure and smaller ones a detachment of the specimen from the support.

Due to the very small relative motion between the specimen and the test device in the evaluation area (Figure 2, V), the friction can be neglected there. Nevertheless, the support surfaces should be treated properly to minimise their friction coefficient. As a result, it can be assumed that the friction does not influence the results significantly.

A test device with a = 80 mm and m_0 = tan(–20°) has been designed and build according to these criteria [16]. The size of the specimens is $L \times B = 83.5 \times 15$ mm^2.

3.1.2 Test procedure

For testing a specimen is inserted in the test device, see Figure 2(b). While assuring a deflection towards the supporting plates, the upper support plate is displaced until the material-dependent critical force is reached or the complete specimen touches the supporting plates. Afterwards, the clamping brackets have to be attached to the supporting plates, see Figure 2(c). The clamping force shall be big enough to assure a clamping effect, but small enough not to damage the specimen. Otherwise, the specimen can fail in the clamping region under smaller loads.

While measuring the deformation and the applied force, F_{test}, the upper support plate is displaced with a constant speed of v_x = 0.5 mm/min. Higher or lower speeds are also possible. Furthermore, a two-column guidance is used to minimise z- and y-displacements to a negligible level.

The digital image correlation system ARAMIS (by GOM mbH, Germany) is applied to measure the specimen deformation in the evaluation area directly, see Figure 2(d). Therefore, it is possible to calculate the stress-strain relation in x-direction and the x-strain-y-strain relation.

3.1.3 Applicability

Most paper and paper-like materials can be tested with this compression test device. Besides the investigated papers N636 and APM, papers with a grammage of 100 g/m^2 to 350 g/m^2 and a thickness of 0.15 mm to 0.67 mm have been successfully tested. For tests on materials with a higher or lower bending stiffness, it is possible to adjust the curvature of the test device according to equation 6. Only materials with uneven surfaces or significant inhomogeneities perform poorly, due to an early detachment of the specimen.

3.2 Shear test – shear-frame device

Since the investigated paper is an orthotropic material, a measurement of the shear properties is necessary. In literature, only some few test methods can be found [6]. Shear tests like the Iosupescu [17] and the Arcan test [18] can only be performed on thick or multilayer materials. Furthemore, these methods cause an irregular multi-axial state of stress and are therefore not suitable for the given task. Setterholm et al. describe a torsion test that uses a cylindrical specimen in

[19]. This method is rather complex and a single test device is only applicable to materials with similar bending stiffnesses, which is not the case for the investigated materials. Another approach is the off-axis testing procedure [18]. That is basically a tensile test, for which the machine direction of the paper is tilted about 15° or 45° to the direction of loading. This method is limited for linear-elastic materials and therefore not suitable for the developed paper-like materials.

3.2.1 Developing a shear-frame device

The literature survey revealed that a shear-frame type test seems to be the most suitable. Hähnel and Wolf [20] developed such a device which is applicable to paper and paper-like materials. This test method has been adapted and enhanced.

Figure 3(a) shows a drawing of the undeformed test region. If a displacement Δx is applied, the specimen is subjected to a shear force, see Figure 3(b). The shear-frame in Figure 3(c) consists of four frame parts with the same edge-length that are connected by pins. The clamping brackets connect the specimen with each frame part. The size of the quadratic testing area is $b \times b = 10 \times 10$ mm^2. These dimensions proved to be a good compromise between a manageable specimen size and a low probability of buckling failure for thicker materials.

Investigations have shown that the very thin paper sheets tend to buckle. Therefore, a new specimen support was developed, where pins connect a supporting plate to the mid-points of the mid-frame parts. Hence, the rotation of the supporting plate is restricted and the movement of the frame parts is permitted. Figure 3(a)

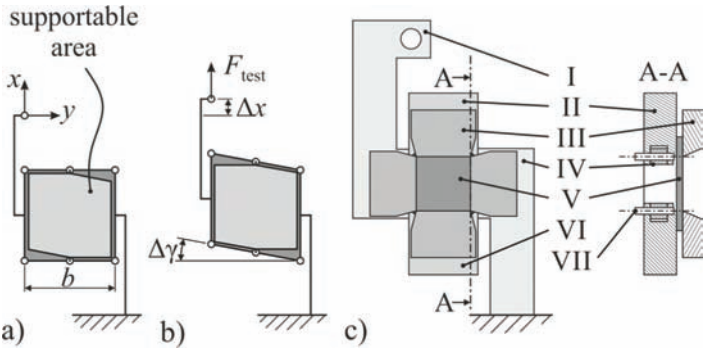

Figure 3. Theory and construction of the shear-frame test device: (a) undeformed test state; (b) deformed test state; (c) the front and section view show the movable frame part (I), the mid-frame part (II) (VI), the clamping brackets (III), the fixed frame part (IV), the specimen (V) and the pin (VII).

and 3(b) shows the resulting supportable area for the undeformed and deformed test state. For a maximum displacement $\Delta\hat{x}$ the maximum unsupported line length is approximately $\Delta\hat{x}/2$. For the frame used for testing, $\Delta\hat{x}$ has been chosen to 1.25 *mm*.

3.2.2 Test procedure for materials without buckling failure

A specimen is inserted in the test device. The clamping brackets fix the specimen to the frame parts. For materials with a high bending stiffness, the use of supporting plates is not necessary. While measuring the deformation and the force F_{test}, the moveable part of the frame is displaced with a speed of $v_x = 0.5$ mm/min. However, higher or lower displacement speeds are also possible.

A digital image correlation (DIC) system has been used to measure the shear-deformation directly. Therefore, it is possible to calculate the shear stress-strain relation. Furthermore, the digital image correlation method permits to decide if a specimen buckles, since the out-of-plane deformation can be evaluated.

3.2.3 Test procedure for materials with buckling failure

For specimen with a very low bending stiffness a two-staged approach is necessary. The first part is equal to the test procedure described in Section 3.2.2. The only difference is that additionally to the deformation measurement on the specimen also the displacement of the shear-frame Δx has to be determined. Both measurements yield a shear strain

$$\gamma_{\text{DIC}} \text{ and } \gamma\Delta_x. \tag{9}$$

Due to clamping effects, tolerances in the bearing and the non-linear behaviour of paper or paper-like materials $\gamma\Delta_x$ is in general larger than γ_{DIC}. Consequently, a correlation factor can be determined in a parametric form by

$$f_c(t) = \left.\frac{\gamma_{\text{DIC}}(t)}{\gamma_{\Delta x}(t)}\right|_0^{t_B}. \tag{10}$$

t_B is defined as the point at which buckling begins to occur. It can be determined by out-of-plane measurements using digital image correlation methods. f_c is a material specific function and can be approximated by a constant value between 0.6 and 0.9.

In the second part, the specimens are tested with the support plates. Therefore, it is not possible to measure the shear strain directly. Instead, it has to be

determined from the displacement of the shear-frame using the correlation function:

$$\gamma_c = f_c \cdot \gamma\Delta_x(t) \tag{11}$$

This procedure permits to determine the shear stress-strain relation for very thin and flexible specimens.

3.2.4 Applicability

The materials that are mentioned in section 3.1.3 have also been tested with the shear-frame device. For thin papers of approximately 0.15 mm, the test procedure according to section 3.2.3 have been used. Thicker materials were tested without support plates. Additionally, shear tests on wood veneers have been carried out successfully. The testing of very stiff materials like carbon fibre reinforced plastics is difficult, since the parts of the shear-frame device may deform. This can influence the results. In conclusion, most papers and paper-like materials can be tested with this shear-frame device.

4 PAPER TESTING

Tensile tests according to the standard DIN1924-2 as well as compression and shear tests based on the developed methods have been carried out to characterise APM and N636®. Figure 4 shows the compression test device and shear test device with and without support plates.

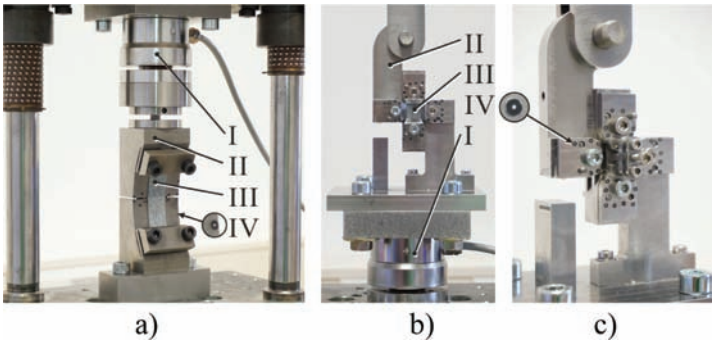

Figure 4. Compression tests (a) and shear tests without (b) and with support plates (c): I – load cell, II – test device, III – specimen and VI – tracking points.

A number of 8 specimens were tested for each loading case. Figure 5(a) and 5(b) show the stress-strain curves determined by tensile and compression tests in machine- and cross-direction for both materials. The obtained stress-strain curves are somewhat non-linear for all tests. Compared to the benchmark material N636® both the compression and the tensile strength of APM is lower.

The results from shear tests with support plates are shown in Figure 5(c) for APM and 5(d) for N636®. The shear strain has been corrected using the experimentally determined correlation factor f_c = 0.65. The diagrams clearly show a non-linear trend of the stress-strain curves that is for shear loading more distinct than for the other load cases. Furthermore, the shear strength of APM is lower than for N636®.

Numerical simulation methods require material models, which describe the mechanical behaviour of the used material. For paper and paper-like materials, Mäkelä and Östlund [21] proposed a model, which is based on a modified Ramberg-Osgood relation. The strain is divided in an elastic and a plastic part where the latter is characterised by the hardening modulus E_0 and the hardening exponent n.

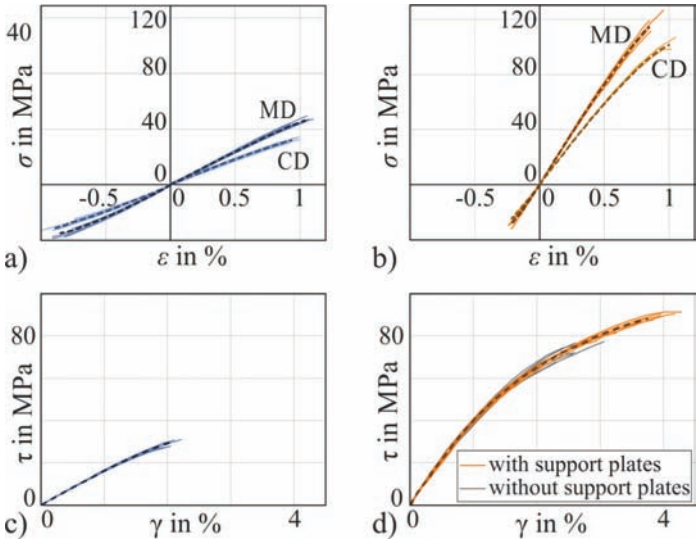

Figure 5. Stress-strain relation of (a) APM and (b) N636® in machine- and cross-direction in the compressive and tensile load regime and shear stress-strain relation of (c) APM and (d) N636® (—— test results,– – – average curve).

$$\varepsilon = \frac{\sigma}{E} + \left(\frac{\sigma}{E_0} \right)^n \tag{12}$$

This basic model has been adapted to the investigated materials by modifying the yield surface and adding appropriate failure criteria [22]. Derived from equation 12 the resulting stress-strain relations are:

$$\varepsilon_{\mathrm{MD}} = \frac{\sigma_{\mathrm{MD}}}{E_{\mathrm{MD}}} + \left(\frac{\sigma_{\mathrm{MD}}}{E_0} \right)^n \tag{13}$$

$$\varepsilon_{\mathrm{CD}} = \frac{\sigma_{\mathrm{CD}}}{E_{\mathrm{CD}}} + \left(K_{\mathrm{CD}} \cdot \frac{\sigma_{\mathrm{CD}}}{E_0} \right)^n \tag{14}$$

$$\varepsilon_{\bar{\mathrm{M}}\mathrm{D}} = \frac{\sigma_{\bar{\mathrm{M}}\mathrm{D}}}{E_{\mathrm{MD}}} + \left(K_{\bar{\mathrm{M}}\mathrm{D}} \cdot \frac{\sigma_{\bar{\mathrm{M}}\mathrm{D}}}{E_0} \right)^n \tag{15}$$

$$\varepsilon_{\bar{\mathrm{C}}\mathrm{D}} = \frac{\sigma_{\bar{\mathrm{C}}\mathrm{D}}}{E_{\mathrm{CD}}} + \left(K_{\bar{\mathrm{C}}\mathrm{D}} \cdot \frac{\sigma_{\bar{\mathrm{C}}\mathrm{D}}}{E_0} \right)^n \tag{16}$$

$$\gamma = \frac{\tau}{G} + \left(K_{\tau} \cdot \frac{\tau}{E_0} \right)^n \tag{17}$$

For the complete characterization of the material behaviour, four elastic and six plastic parameters as well as five strength values are required. These parameters have been determined from the experimental data for APM and N636® using a curve fitting algorithm. The obtained values are summarized in Table 2. Furthermore, the table gives the thickness and grammage of both materials determined according to the standards ISO 534 [23] and ISO 536 [24].

Additionally, Table 2 shows that the weight specific elastic parameters, the tensile strengths and the shear strength of APM are 17–33% lower than the values of N636®. Nevertheless, the weight specific compression strength of APM is 138–152% higher. The compression and shear strength of the cell wall material have a high influence on the load carrying capabilities of sandwich cores. Hence, an increase leads to increasing core compression and shear strength. Finally, the definition

$$S = \frac{Et^3}{12} \tag{18}$$

Table 2. Experimentally determined material parameters for APM and N636®: (a) general and weight specific elastic parameters, (b) plastic parameters, (c) weight specific strengths and bending stiffness

(a)		t/mm	$\bar{m}/\frac{\mathrm{g}}{\mathrm{m}^2}$	ν	$\frac{E_{MD}t}{\bar{m}}/\frac{\mathrm{kN\,m}}{\mathrm{g}}$	$\frac{E_{CD}t}{\bar{m}}/\frac{\mathrm{kN\,m}}{\mathrm{g}}$	$\frac{Gt}{\bar{m}}/\frac{\mathrm{kN\,m}}{\mathrm{g}}$
	APM	0.728	366.2	0.390	9.471	7.395	3.335
	N636	0.148	165.5	0.390	13.52	11.00	4.306
(b)		$E_0/\frac{\mathrm{N}}{\mathrm{mm}^2}$	n	K_{CD}	$K\tau$	K^{-}_{MD}	K^{-}_{CD}
	APM	231.9	4.516	1.463	2.188	1.522	1.704
	N636	548.7	4.422	1.308	2.560	2.770	2.886
(c)		$\frac{\hat{\sigma}_{MD}t}{\bar{m}}/\frac{\mathrm{N\,m}}{\mathrm{g}}$	$\frac{\hat{\sigma}_{CD}t}{\bar{m}}/\frac{\mathrm{N\,m}}{\mathrm{g}}$	$\frac{\hat{\sigma}_{\bar{M}D}t}{\bar{m}}/\frac{\mathrm{N\,m}}{\mathrm{g}}$	$\frac{\hat{\sigma}_{\bar{C}D}t}{\bar{m}}/\frac{\mathrm{N\,m}}{\mathrm{g}}$	$\frac{\hat{\tau}\,t}{\bar{m}}/\frac{\mathrm{N\,m}}{\mathrm{g}}$	$\frac{Et^3}{12}/\mathrm{N\,mm}$
	APM	89.76	63.79	–66.80	–57.44	57.41	153.0
	N636	107.5	95.07	–26.54	–24.18	79.19	4.09

yields, according to Table 2, that APM has a 37 times higher bending stiffness than N636®. Obviously, cores made out of the adapted paper-like material will not fail because of buckling cell walls in the same way as N636® cores.

5 CONCLUSION

A novel three-layered paper-like material (APM) for honeycomb- and foldcores has been developed. While the face layers consist of carbon fibres and aramid fibrids, in the middle layer the light-weight filler Perlit® is added. For benchmark purpose N636® has been selected as reference material, because it is already used as wall material for state of the art sandwich cores.

The aim for further research was to determine the mechanical properties of complete cores using numerical simulation. Therefore, a complete characterisation of the adapted paper-like material (APM) and the N636® reference material was necessary. Hence, new and enhanced testing devices had to be developed. The compressive properties were determined by a single-curved compression test and the shear properties by a modified shear-frame. By means of these test methods as well as standardised tests, the stress-strain relations under tensile, compression and shear loads were determined for both materials. The obtained experimental data confirmed that the chosen approach to improve the mechanical

performance of core wall materials by novel multi-layered paper-like materials had been successful.

ACKNOWLEDGEMENT

The research work was funded by the Federal Ministry for Economic Affairs and Energy (BMWi), following a decision of the German Bundestag. This financial support is gratefully acknowledged.

REFERENCES

1. F. Hähnel. 'Ein Beitrag zur Simulation des Versagens von Honigwaben aus Meta-Aramid-Papier in schlagbelasteten Sandwich-Strukturen,' Doctoral Dissertation. Faculty of Mechanical Science and Engineering, TUD, Dresden, 2016.
2. T. Bitzer. *Honeycomb Technology*, London: Chapman & Hall, 1997.
3. I. M. Zakirov, A. Nikitin, K. Alexeev and C.F. Mudra. Foldcore structures: performance, technology and production. In Proc. *SAMPE EUROPE*, International Conference, Paris, 2006.
4. Standard – ISO 1924–2: Paper and board – Determination of tensile properties – Part 2: Constant rate of elongation method (20 mm/min), 12 2008.
5. C. Fellers. 'The Significance of Structure on the Compression Behaviour of Paper.' Doctoral Dissertation. KTH, Stockholm, 1980.
6. R. E. Mark. *Handbook of Physical and Mechanical Testing of Paper and Paperboard*, Vol. 1, New York: Marcel Dekker Inc., 1983.
7. Standard – Tappi Useful Method 811: The Concora fluted crush test for corrugating medium.
8. Standard – ISO 12192: Paper and board – Determination of compressive strength – Ring crush method, 09 2011.
9. V. C. Setterholm and R. O. Gertjejansen. Method for measuring the edgewise compressive properties of paper, *Tappi* **48**(5):308–312, 1965.
10. S. Calvin and C. Fellers. A new method for measuring the edgewise compression properties of paper, *Svensk Papperstidn* **78**(9):329–332, 1975.
11. Standard – Tappi Useful Method 801: The Concora liner (edge) crush test (CLT).
12. C. Fellers, A. de Ruvo, J. Elfstorm and M. Htun. Edgewise compression properties. A comparison handsheets made from pulps of various yields, *Tappi* **63**(6):109–112, 1980.
13. D. E. Gunderson. A comparison of three methods for determining the edgewise compressive properties of paperboard, *Appita* **37**(4):307–313, 1984.
14. R. S. Seth and R. M. Soszynski. An evaluation of methods for measuring the intrinsic edgewise compressive strength of paper, *Tappi* **62**(10):124–127, 1979.
15. D. E. Gunderson. Edgewise compression of paperboard: A new concept of lateral support, *Appita* **37**(2):137–141, 1983.

16. A. Bugiel, P. Reichenbach, F. Hähnel and K. Wolf. Prüfvorrichtung für Druckfestigkeit dünnwandiger Materialien. Patent DE 102015100467 A1 pend., 2016.
17. P. B. Gning, D. Delsart, J. M. Mortier and D. Coutelliera. Through-thickness strength measurements using Arcan's method, *Composites: Part B* **41:**308–316, 2010.
18. J. Xaviera, N. Garridob, M. Oliveirab, J. Moraisa, P. Camanhoc and F. Pierrond. A comparison between the Iosipescu and off-axis shear test methods for the characterization of Pinus Pinaster Ait, *Composites: Part A* **35:**827–840, 2004.
19. V. C. Setterholm, R. Benson and E. W. Kuenzi. Method for measuring edgewise shear properties of paper, *Tappi* **51**(5):196–202, 1968.
20. F. Hähnel and K. Wolf. Vorrichtung für die mechanische Werkstoffprüfung zur Bestimmung der Schubkennwerte von Werkstoffen. Patent DE 102010006163, 2011.
21. P. Mäkelä and S. Östlund: Orthotropic elastic–plastic material model for paper materials, *International Journal of Solids and Structures* **40**:5599–5620, 2003.
22. A. Bugiel, F. Hähnel, T. Kuntzsch and J. Strauß. Analyse und Simulation mechanischer Eigenschaften bei der Entwicklung adaptierter papierartiger Werkstoffe für Falt- und Honigwabenkerne. PTS-ILR-final report, IGF 18256 BG, 2017.
23. Standard – ISO 534: Determination of thickness, density and specific volume, 02 2012.
24. Standard – ISO 536: Paper and board – Determination of grammage, 11 2012.

Transcription of Discussion

ENHANCED TEST DEVICES FOR THE DEVELOPMENT OF NOVEL PAPER -LIKE MATERIALS FOR SANDWICH-STRUCTURES

Alexander Bugiel,[1] *Falk Hähnel,*[1] *Klaus Wolf,*[1]
Johann Strauß[2] *and Timo Kuntzsch*[3]

[1] Institute of Aerospace Engineering, Technische Universität Dresden, Germany
[2] Papiertechnische Stiftung Munich, Germany
[3] Papiertechnische Stiftung Heidenau, Germany

Artem Kulachenko KTH Royal Institute of Technology

You have developed two interesting tests and one of them is for measuring shear properties of the paper material. There is an alternative method of acquiring the shear stiffness of paper by making the experiment in a 45 degree angle.

Alexander Bugiel Technische Universität Dresden

Yes, I know.

Artem Kulachenko

Have you compared the result of your tests with this method?

Alexander Bugiel

We haven't done it because you don't have uniform stress distribution over the whole length of the specimen. You have the clamping effects and another stress distribution as in the middle. Furthermore, you have a slight tilting of the specimen and you can't use it for isotropic materials and we wanted to use our test

device for isotropic materials, therefore we haven't considered the 45, or 10 degrees test method.

Gil Garnier Monash University

Very interesting. Why do you use a filler, why perlite and how much do you use?

Alexander Bugiel

We use a filler to increase the distance of the face-sheets, so that it has a higher bending stiffness. It's almost the same as for sandwich structures by increasing the height or by increasing the distance of the face-sheets without increasing weight of the material significantly. In the same manner, we can increase bending stiffness significantly. As you can see in this simple example. That is why we use the filler and we use perlite because it is non-combustible and we don't want it to have organic materials that can burn, or smoke and because it is hard in air cabin design to use such material.

Gil Garnier

Inorganic fillers add weight. Is that an issue for airplane application? Also, fillers typically act as stress initiators in a composite. Is that an issue? Is that not a lot of weight to act as a stress initiator in a composite?

Alexander Bugiel

As a stress initiator, I don't think so.

Gil Garnier

Do you have very weak adhesion between inorganic and fibrous resin?

Alexander Bugiel

Yes, maybe but these materials are, as you can see it here, impregnated with phenolic resin completely. So the phenolic resin connects the fibres and fillers and fibrils.